Simulations of nanosecond laser self-focusing and channeling in under-dense magnetised plasmas

Contact *martin.read@york.ac.uk*

M. P. Read

York Plasma Institute
University of York, Heslington, York, YO10 5DQ

Blackett Laboratory
Imperial College London, London, SW7 2AZ

R. J. Kingham

Blackett Laboratory
Imperial College London, London, SW7 2AZ

P. A. Norreys

Clarendon Laboratory
University of Oxford, Parks Road, Oxford, OX1 3PU

Central Laser Facility
Rutherford Appleton Laboratory, Harwell Science and Innovation Campus, Didcot, Oxfordshire, OX11 0QX

Introduction

In recent years there has been a growing interest in transport dynamics of laser-plasmas in the presence of magnetic fields. In such plasmas, strong magnetic fields (~100T) can be self-generated by the $\nabla n_e \times \nabla T_e$ (Biermann battery) mechanism or externally applied to the system. Magnetic fields are being experimentally utilised for the purposes of easing the path to ignition in ICF (e.g., improving laser-plasma coupling in hohlraum targets [1] and increasing fusion yield in direct-drive experiments [2]), for their benefits to plasma wave-guide formation [3] and for the study of fundamental plasma physics.

The presence of a magnetic field in the plasma complicates electron transport dynamics as heat-flow across field lines is suppressed but magnetic field evolution is affected by heat-flow via Nernst advection. Under appropriate conditions, a range of magnetised transport phenomena are present in laser-plasmas. These transport effects in turn modify the hydrodynamic evolution of the plasma, the thermal profile and can lead to instabilities. Additionally, magnetic fields can affect temperature scale-lengths and determine whether the local approximation is fulfilled which has ramifications on the validity of fluid codes. For this reason, a complete model of electron transport in the presence of B-fields under such conditions is vital to the simulation and interpretation of laser-plasma experiments.

Laser propagation in plasmas is governed by the refractive index which is determined by the density profile as $\eta \propto (n_e / n_{cr})^{1/2}$. This work presents simulations aiming to understand the links between laser propagation and plasma evolution when a full range of magnetised transport phenomena are accounted for.

Code Development

Electron transport in the presence of a magnetic field is governed by the Braginskii transport equations [4] for Ohm's law and heat-flow **q**, as shown below, where α^c, β^c, and κ^c are the normalised resistivity, thermoelectric and thermal conductivity tensors and τ is the electron-ion collision time.

$$en_e\left(\mathbf{E}+\mathbf{C}\times\mathbf{B}\right)=-\nabla P_e+\mathbf{j}\times\mathbf{B}+\frac{m_e}{e\tau_B}\underline{\underline{\alpha}}^c\cdot\mathbf{j}-n_e\underline{\underline{\beta}}^c\cdot\nabla T_e$$

$$\mathbf{q}=-\frac{n_e\tau_B T_e}{m_e}\underline{\underline{\kappa}}^c\cdot\nabla T_e-\underline{\underline{\beta}}^c\cdot\mathbf{j}\frac{T_e}{e}$$

The electric field **E** determined by Ohm's law can be combined with Faraday's law to give an induction equation describing the evolution of the magnetic field **B** within the plasma due to a number of magnetised transport phenomena. The component of the thermoelectric term ($\underline{\beta}^c \cdot \nabla T_e$) in Ohm's law perpendicular to both the magnetic field and temperature gradient gives rise to the Nernst effect - an advection of magnetic fields along with heat-flow down temperature gradients – which is particularly important to the work presented here. In previous VFP simulations [5], Nernst field advection has been shown to have a dramatic effect on magnetic field evolution, in turn leading to changes in the density and thermal profiles and leading to the re-emergence of non-local transport in systems which were previously localised. Due to the intricate coupling between magnetised electron transport, plasma hydrodynamics and a dynamically evolving laser beam, a numerical approach to modelling the problem is taken.

The interaction between a long-pulse (ns) beam and an under-dense magnetised plasma is simulated using CTC [6], a 2D classical transport code including the Braginskii electron transport equations, and IMPACT [7], a fully implicit 2D VFP code including magnetic fields and implicitly incorporating magnetised electron transport. The use of both codes is beneficial as they share the same geometry – 2D slab Cartesian (x-y) with a B-field component (B_z) perpendicular to the plane of simulation. CTC, the fluid code, benefits from a relatively fast run-time and allows for the toggling of different plasma transport phenomena. IMPACT is computationally expensive but provides a more sophisticated treatment able to account for non-local effects and non-Maxwellian distribution functions. The laser is accounted for using a newly developed paraxial wave solving module based on the paraxial wave treatment described by Sentis [7]. The laser solving module is coupled to both codes via IB heating and the plasma refractive index. The addition of the laser solver allows for the dynamics of the laser pulse to be modeled as it propagates through an evolving plasma.

Simulations

Under-dense laser-plasmas under varying conditions were simulated using the fluid and VFP codes. For the results presented here, the simulation domain was ~1 mm^2 and the beam propagation was modelled over timescales of ~1 ns. The initial plasma temperature was T_{e0} = 20 eV, the initial plasma density was $n_{e0} = 1.5 \times 10^{19}$ cm^{-3} and magnetic fields ranged from 0 – 6 T. The laser had intensity $I_L = 3.9 \times 10^{14}$ Wcm^{-2}, a wavelength of λ_L = 1054 nm and a FWHM of φ = 10 μm.

Simulations were performed primarily using CTC to explore parameter space and the effects of various terms in the transport equations – specifically the Nernst effect and Righi-Leduc heat-flow – were investigated by toggling terms in the transport equations. IMPACT was used to look for non-local and kinetic effects and validate the results of the fluid model. The simulations performed were limited by computing power, as simulating macroscopic volumes of plasma over nanosecond timescales using kinetic codes is computationally expensive. The magnetothermal [6] instability – an instability resulting from the interplay between Nernst advection and Righi-Leduc heat-flow –

leads to unstable temperature and magnetic field profiles and hindered the exploration of a wider parameter space.

Results and Discussion

Simulations undertaken using CTC show significant changes in laser focusing dynamics over a 2 mm distance when Nernst advection was switched on / off. Figure 1 shows the intensity profiles with (upper) and without (lower) Nernst advection for an initial magnetic field of B = 6 T after 350ps of plasma evolution.

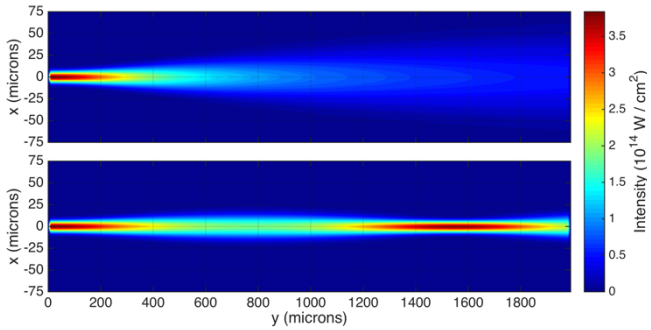

Figure 1: Changes to the intensity profile after ~350 ps. When the Nernst effect is enabled (upper), the laser defocuses whereas when it is disabled (lower), the beam demonstrates self-focusing due to plasma channel formation.

With Nernst advection the laser defocuses as it propagates, whereas without Nernst advection, the beam is channeled resulting in a continuous focusing and defocusing behavior. These results can be explained by observing the plasma density, temperature and magnetic field profiles, transverse lineouts (1 mm into the domain) of which are shown in figure 2. Nernst advection (closed circles) leads to a rapid evacuation of 90% of the magnetic field from the central heated region after 350 ps whereas when it is not accounted for (open circles), only ~25% of the field escapes. The changes in the magnetic field lead to the central region becoming un-magnetised, allowing for un-suppressed heat-flow and a wider, flatter temperature profile.

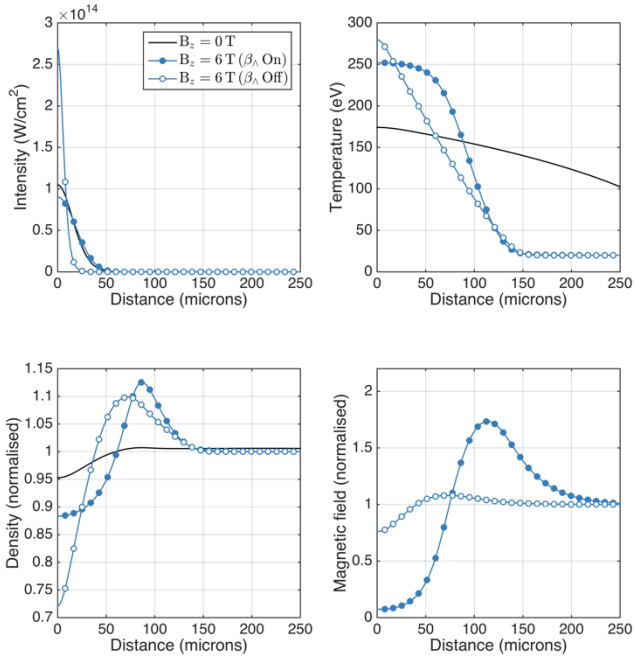

Figure 2: Laser intensity and plasma temperature, density and B-field lineouts 1 mm into the domain after 350 ps.

This in turn affects the thermal pressure and leads to a significantly altered plasma density – a shallow, broad profile when the Nernst effect is enabled, and a narrow, deep profile when it is disabled. In the broad profile, the beam can defocus. In the narrow profile, the beam is continuously channeled.

Figure 3 shows a comparison of the intensity profiles after ~350 ps for the fluid code (CTC) and the VFP code (IMPACT).

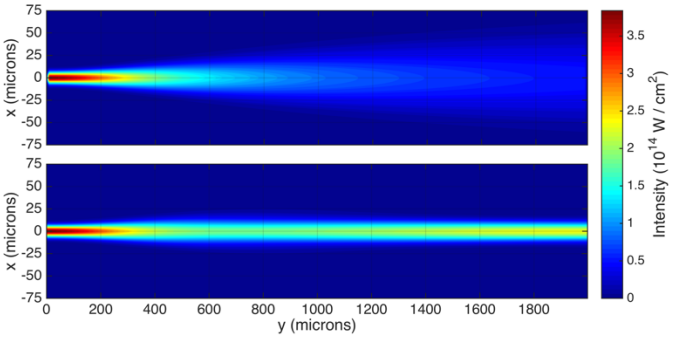

Figure 3: Intensity profiles in the fluid and VFP codes after ~350 ps. The full fluid (upper) codes shows a defocusing laser beam whilst the VFP model (lower) exhibits beam self-focusing behavior.

Under these parameters, CTC (including Nernst advection) produces a defocusing beam whilst the full kinetic approach using IMPACT results in a channeled beam self-focusing over the length of the domain. The change in focusing is likely due to non-local effects. Under these conditions the transport in the central heated region of the plasma will be non-local resulting in a decreased heat-flow in the regions of steepest temperature gradient. The fluid code overestimates the heat-flow out of the laser-heated region and also overestimates the Nernst advection resulting in a faster than expected cavitation of the B-field. To correctly match the non-local behavior shown in the VFP code, CTC could make use of a flux limiter for the heat-flow and the field advection. Choice of the correct limiter for Nernst field advection is the subject of ongoing work [9].

Conclusions

Simulations of beam propagation in under-dense magnetised plasma using the fluid code CTC coupled to a paraxial wave solving module have demonstrated interesting laser-focusing phenomena resulting from the feedback of Nernst advected B-field onto the density profile. Kinetic simulations using the VFP code IMPACT show that under these particular conditions the beam defocusing phenomena does not arise as readily and beam channeling behavior is maintained. Previous work with VFP simulations [5] has shown significant changes to B-field and density in kinetic simulations due to the Nernst effect and therefore it is likely that non-local transport has lead to a shift in the threshold beyond which defocusing occurs at these parameters.

Acknowledgements

The computational work presented here is associated with a TAW experiment performed in 2013 (Application No. 12210018). The author would like to acknowledge the funding of the UK EPSRC and the HPC facilities provided by the Imperial College High Performance Computing Service.

References

1. D. S. Montgomery *et al*, Phys. Plasmas **22**, 079901 (2015)
2. P. Y. Chang *et al*, Phys. Rev. Lett. **107** (2011)
3. D. H. Froula *et al*, Plas. Phys. Cont. Fus. **51**, 024009 (2009)
4. S. I. Braginskii, Rev. Plas. Phys. **1**, 205 (1965)
5. C. P. Ridgers *et al*, Phys. Rev. Lett. **100**, 075003 (2008)
6. J. J. Bissell *et al*, Phys. Rev. Lett. **105**, 175001 (2010)
7. R. J. Kingham and A. R. Bell, J. Comp. Phys. **194** (2004)
8. R. Sentis, ESAIM **39** (2005)
9. J. J. Bissell, CLF Annual Report '12-13 (2013)